

# physica **p** status **s** solidi **S**

[www.interscience.wiley.com](http://www.interscience.wiley.com)

**reprints**

**physica status solidi <sup>a</sup>**  
[www.pss-a.com](http://www.pss-a.com)  
**applications and materials science**  
Editor's Choice  
Highly efficient all nitride phosphor-converted white light emitting diode  
(Reyna Mueller-Mach et al., p. 1727)  
[www.pss-a.com](http://www.pss-a.com)

**physica status solidi <sup>b</sup>**  
[www.pss-b.com](http://www.pss-b.com)  
**basic solid state physics**  
Current Trends in Electronic Structure: Embedding and Linear Scaling Techniques  
Thomas Beck, and Eduardo Hernández  
**SPECIAL ISSUE**  
[www.pss-b.com](http://www.pss-b.com)

**physica status solidi <sup>c</sup>**  
[www.pss-c.com  
\*\*current topics in solid state physics\*\*  
Resonant luminescence color center ions in wide band gap materials  
forming a pair of charged Frenkel-Seliger pairs  
\(Kobayashi et al., p. 833\)  
\[www.pss-c.com\]\(http://www.pss-c.com\)](http://www.pss-c.com)

**physica status solidi <sup>rrl</sup>**  
[www.pss-rapid.com](http://www.pss-rapid.com)  
**rapid research letters**  
[www.pss-rapid.com](http://www.pss-rapid.com)

# Luminescent and scintillation properties of CsI:Tl films grown by the liquid phase epitaxy method

Yu. Zorenko<sup>\*1,4</sup>, T. Voznyak<sup>1</sup>, R. Turchak<sup>1</sup>, A. Fedorov<sup>2</sup>, K. Wiesniewski<sup>3</sup>, and M. Grinberg<sup>3</sup>

<sup>1</sup>Laboratory of Optoelectronic Materials (LOM), Electronics Department of Ivan Franko National University of Lviv, 107 Gen. Tarnawskiego Str., 70017 Lviv, Ukraine

<sup>2</sup>Institute for Scintillation Materials of NAS of Ukraine, 60 Lenina Ave., 61001 Kharkiv, Ukraine

<sup>3</sup>Institute of Experimental Physics of Gdansk University, 57 Wita Stwoza, 80-952 Gdansk, Poland

<sup>4</sup>Institute of Physics, Kazimierz Wielki University in Bydgoszcz, 85-090 Bydgoszcz, Poland

Received 3 April 2009, revised 3 February 2010, accepted 16 April 2010

Published online 7 July 2010

**Keywords** impurity levels, liquid phase epitaxy, luminescence

\* Corresponding author: e-mail yuriyzorenko@gmail.com, Phone: +380322 394205, Fax: +380 322 448585

CsI:Tl films have been crystallized by the liquid phase epitaxy (LPE) method from CsI:Tl (0.3 mol.%) crystalline salt onto CsI substrates. The luminescent and scintillation properties of CsI:Tl films are systematically compared with the corresponding properties of CsI:Tl (0.3 and 0.03%) crystals grown from the melt. The luminescence of CsI:Tl films and CsI:Tl (0.03%) crystals in the bands peaked at 2.52 and 2.22 eV is related to the radiative relaxation from the weak-off and strong-off configurations of excitons localized around  $Tl^+$  ions, respectively.

Apart from single  $Tl^+$  centers, in highly doped CsI:Tl (0.3%) crystals creation of  $Tl^+$  dimer centers occurs. These centers form the additional emission bands peaked at 2.42 and 1.98 eV related to the weak-off and strong-off configurations of excitons localized around  $Tl^+$  dimer centers. We found that the dominant mechanism of excitation of the strong-off luminescence of localized excitons in CsI:Tl films and crystals is the charge-transfer transition between  $\Gamma^-$  anions and  $Tl^+$  ions in single and dimer centers.

© 2010 WILEY-VCH Verlag GmbH & Co. KGaA, Weinheim

**1 Introduction** The modern digital X-ray and gamma-ray imaging systems are usually based on the crystalline scintillating screens emitting in the visible or UV ranges coupled with the novel detectors (CCD cameras or amorphous silicon arrays) [1]. A wide variety of applications of such devices (nondestructive testing, astronomy, medicine, crystallography and basic physical research) strongly demand the development of series of scintillating screens with high detection efficiency and excellent spatial resolution.

CsI:Tl is a well-known scintillating material that can convert incident X- and  $\gamma$ -rays into visible light with very high conversion efficiency up to 64 000 photons/MeV [2]. Therefore, the preparation of scintillating screens based on thick CsI:Tl crystalline films has been the main topic of activity of several research groups in the last few years [3–8].

The CsI:Tl crystalline films with 5–200  $\mu\text{m}$  thickness were obtained for the first time by a vapor deposition technique onto the (100) cleavage planes of LiF single

crystal and onto the amorphous glass substrate [3]. In both cases columnar morphology of films was observed. The CsI:Tl films grown onto the orienting LiF substrate have single-crystalline structure of columns in (110) and (112) orientations which are not coincident with the orientation of substrate due to the large lattice misfit and weak interaction between the layer and substrate. The oriented columnar CsI:Tl films with thicknesses more than 10  $\mu\text{m}$  demonstrate the scintillation efficiency comparable with that of standard CsI:Tl single-crystalline  $\alpha$ -detector [3, 4].

The high-quality CsI:Tl films have been developed by the specialists of RMD company [5–7] using a vapor deposition technique on a specially designed substrates. The films were grown in the form of oriented microstructured columns with controllable diameter in the 3–5 mm range. The microcolumnar structure of the films suppresses lateral spreading of the scintillation light resulting in superior spatial resolution compared to bulk or polycrystalline scintillators. This allows high spatial

© 2010 WILEY-VCH Verlag GmbH & Co. KGaA, Weinheim

resolution of the screens for applications in medical imaging to be achieved.

In recent work [8], the CsI:Tl thin-film scintillators were also manufactured by the thermal deposition method. The scintillation characteristics of the CsI:Tl thin films were studied by X-ray-excited luminescence for different Tl concentrations between 0.05 and 1.0 mol.%. The wavelength of the main emission peak of films was about of 550 nm. The light intensity increased and the emission peak of X-ray-excited luminescence shifted toward the long wavelength for the higher Tl concentration.

Apart from the thermal deposition, the liquid phase epitaxy (LPE) methods can be also successfully applied for producing high-quality single-crystalline film scintillators of oxide [9, 10] and alkali-halide compounds [11] for application in medical imaging and nondestructive testing [1]. Such scintillating films are used in environmental monitoring for detection of  $\alpha$  and  $\beta$  particles as well [12]. The LPE methods also allow the development of hybrid “all solid-state scintillators”. Namely, the LPE methods can be applied for creation of the “phoswich”-type scintillators containing the bulk single-crystal substrate-scintillator for registration of  $\gamma$ -quanta and LPE-grown film scintillator for detection of  $\alpha$  and  $\beta$  particles [12] (for instance, CsI:Tl film, grown by the LPE method on the CsI:Na substrate). However, to our knowledge, the data related to the growth and luminescent properties of CsI:Tl films prepared by LPE methods are completely absent up to now. Therefore, the aim of this work was crystallization and comparative study of the luminescent and scintillation properties of CsI:Tl thin crystalline films, grown by the LPE method, with their single-crystal analogs, grown by Bridgman methods, using the time-resolved luminescent spectroscopy of crystals and films under excitation by synchrotron radiation (SR) with energy in the 3.6–9 eV range.

It is important to note that the luminescence and scintillation properties of well-known phosphors usually substantially depend on the methods of their preparation. Specifically, single crystals and thin crystalline films of oxide [9, 10] and alkali-halide compounds [11], grown from melt by the Czochralski or Bridgman methods and melt solution by the LPE method, respectively, show the significantly different luminescent properties. These differences are caused by: (i) the highest content of intrinsic substitution-type and vacancy-type defects in crystals, grown from the melt at high temperatures [13, 14] in comparison with the films, crystallized from melt solutions

at significantly lower temperatures [9, 10]; (ii) the presence of flux impurities in the case of crystallization of the films [9, 10]; (iii) the differences in the segregation coefficient of activators for both methods of crystallization [10]. In our work, we try to find such differences in the luminescent properties of CsI:Tl bulk crystals and LPE-grown films and to explain the reasons for such differences.

## 2 Growth of crystals and films and their light yield

Two CsI:Tl crystals were grown by the Stockbarger–Bridgman method from CsI salt of 5 N purity in quartz ampoules in the  $10^{-3}$  Torr vacuum atmosphere at 623 °C with a growth velocity of 2 mm/h. The concentration of Tl dopant in the melt was 0.3 and 0.03 mol.%, respectively. The Tl concentration of 0.225 at.% in the CsI:Tl (0.3%) crystal was determined by electron probe microanalyses (EPMA) using SEM JEOL 6420 equipped by JXA-8612 MX setup. Thus, the segregation coefficient of  $Tl^{+}$  ions in our CsI:Tl crystals, grown from the melt, is very high ( $\sim 0.75$ ) due to the relatively close values of the ionic radii of  $Cs^{+}$  (1.74 Å) and  $Tl^{+}$  (1.59 Å) ions for the eight-fold coordination [15].

CsI:Tl films were crystallized from aqueous-alcoholic solution (a mixture of water with ethyl alcohol) of preliminary crystallized CsI:Tl (0.3 mol.%) salt by the method of slow reduction of temperature. The content of the aqueous-alcoholic solution was characterized by the following molar coefficients:  $Z_1 = C_2H_5OH/H_2O = 0.4$ ;  $Z_2 = CsI/H_2O + C_2H_5OH = 0.29\text{--}0.36$ ;  $Z_3 = Cs/I = 1.0$ ,  $Z_4 = Tl/CsI = 0.003$ . The polished plates of undoped CsI crystals were used as substrates. Deposition of CsI:Tl films was carried out by lowering the solvent's temperature in the two temperature ranges: 29–25 and 40–37 °C. The conditions of crystallization of crystals and films and their light yield (LY) are summarized in Table 1. The thickness of the obtained SCF was in the 16–30  $\mu m$  range. The growth rate of the films was equal to 0.5–2.0 and even 4.4  $\mu m/min$  for the chosen temperature ranges. The Tl concentration in the crystals in the growing films was in the 0.025–0.037 at.% range. Thus, due to lower growth temperature of LPE crystallization, the segregation coefficient of  $Tl^{+}$  ions in CsI:Tl films (0.083–0.123) is lower by approximately one order of magnitude than in the case of CsI:Tl crystal growth from the melt. For this reason, the  $Tl^{+}$  content in CsI:Tl films was close to the activator concentration in CsI:Tl (0.03%) crystal.

The CsI:Tl films after crystallization have different structural quality. The perfection of the films strongly

**Table 1** Conditions of CsI:Tl crystals and films crystallization and their scintillation properties:  $T_g$  is the growth temperature;  $f_g$  is the growth rate; LY is the relative LY (%) under excitation by  $\alpha$  particles of  $Pu^{239}$  (5.15 MeV) sources;  $\Delta E$  (FWHM) is the energy resolution (%);  $h$  is the crystal/film thickness.

content	$T_g$ , °C	$f_g$	$h$ , $\mu m$	LY, %	$\Delta E$ (FWHM, %)
CsI:Tl (0.3%) crystal	621	2 mm/h	500	100%	6.5
CsI:Tl films	40–37	4.4 $\mu m/min$	18	82	19.8
CsI:Tl films	29–25	0.5–2.0 $\mu m/min$	16–30	58–75	22.3–30%

depends on the quality of preparation of the substrate surface; namely, on the sufficient degree of removal of the broken layers induced by mechanical polishing, as well as the temperature of growth. Specifically, the films grown in the 25–29 °C range have polycrystalline-like structure with rough surface. Nevertheless, the films grown in the 40–37 °C range already have large single-crystalline areas with slightly mirror-like surface. Thus, increases in the values of  $T_g$  and  $f_g$  result in significant improvement of the structural perfection of the films. The XRD patterns ( $\text{CuK}\alpha$ ,  $E_{\text{eff}} = 8 \text{ keV}$ ) of the films grown in the mentioned temperature ranges (Fig. 1) confirm this assumption. Specifically, the XRD pattern of the film grown in the 40–37 °C range shows preferable growth of the crystalline film in the (110) plane (curve 2).

The LY of radioluminescence (RL) and energy resolution  $\Delta E$  (FWHM, %) measurements of CsI:Tl crystals and films were performed using a detector based on FEU-110 PMTs with the maxima sensitivity in the range of about 450 nm, and a multichannel single-photon counting system in a time interval of 0.5  $\mu\text{s}$  under excitation by  $\alpha$  particles of  $\text{Pu}^{239}$  sources (5.15 MeV). The LY of RL of CsI:Tl films, grown in the 29–25 and 40–37 °C temperature ranges, was 73–75% and 82%, in comparison with the LY of CsI:Tl (0.3%) crystals. Thus, increasing the temperature of growth as well as the growth rate of films leads to raising their LY (Table 1). Such an increase in the LY most probably is connected with increasing of the structural perfection of films as well as with some increase of  $\text{TI}^+$  content in the films, grown at higher temperature. At the same time, due to some inhomogeneity of CsI:Tl polycrystalline-like films their energy resolution  $\Delta E$  (FWHM, %) was significantly lower (19.1–22.3%) in comparison with the energy resolution of CsI:Tl crystals (6.5%) (Fig. 2).

**3 Luminescent properties of CsI:Tl films and crystals** Comparative analysis of the time-resolved intrinsic and impurity-related luminescence of CsI:Tl films and crystals has been performed at 10 K under excitation by

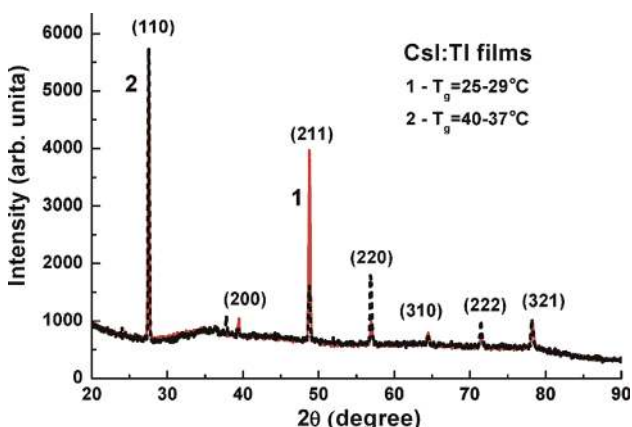


**Figure 1** (online color at: www.pss-a.com) XRD ( $\text{CuK}\alpha$ ) pattern of the CsI:Tl films grown in the 25–29 °C (1) and 40–37 °C (2) ranges (see Table 1).

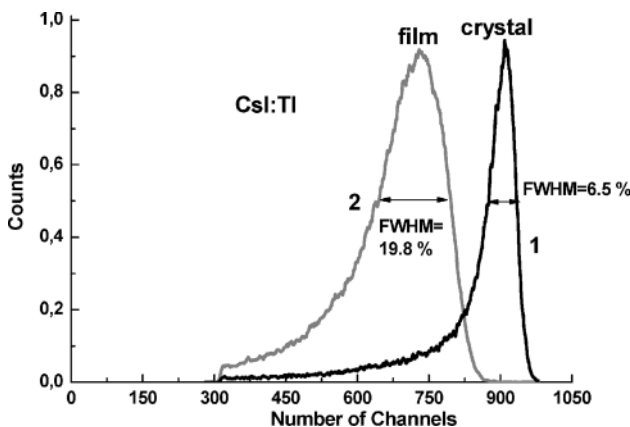


**Figure 2** Amplitude distribution of scintillation pulse from CsI:Tl crystals (1) and films (2) under excitation by  $\alpha$  particles of  $\text{Pu}^{239}$  sources (5.15 MeV). FWHM values for crystals and films are indicated.

pulsed (0.127 ns) SR at Superlumi station (HASLAB at DESY) with an energy of 3.7–10 eV. The emission and excitation spectra were both measured in the integral regime and in the 1.2–6 ns and 150–200 ns time intervals (fast and slow components, respectively) in the limits of SR pulse with a repetition time of 200 ns. The excitation spectra were corrected for the spectral transmittance of the Al grating and the intensity of the SR beam; but emission spectra were not corrected. The decay kinetics of the luminescence under excitation by SR was measured in the 0–200 ns time ranges at 10 K. However, due to the narrow observation time gate (200 ns) we also measured the decay kinetics of the luminescence of CsI:Tl crystal and films in IEP Gdansk University in the wider (0–2  $\mu\text{s}$ ) time range under excitation at 4.27 eV in the A-band band of  $\text{TI}^+$  ions by the Nd:YAG pulse laser pumped by the optical parametric generator PG401/SH. The luminescence was spectrally separated with a Bruker Optics 2501S model monochromator and registered at 300 K using a Hamamatsu C4334-01 model streak camera.

The luminescence spectra of CsI:Tl film (3) and crystals with high (1) and low (2)  $\text{TI}^+$  concentration at 10 K are shown in Fig. 3 under excitation by SR with an energy of 13.75 eV in the range of interband transitions (a) and with an energy of 4.5–4.28 eV in the range of A-absorption band of  $\text{TI}^+$  ions (b). Similarly to CsI:Tl (0.03 at.%) crystal, CsI:Tl film under excitation by SR with an energy of 13.75 eV in the range of CsI interband transitions at 10 K possess the luminescence of self-trapped excitons (STE) in the low-intensity band with  $E_{\text{max}} = 4.26 \text{ eV}$  and the intensive band with  $E_{\text{max}} = 3.66 \text{ eV}$  ( $\sigma$ - and  $\pi$ -components, respectively) (Fig. 3a, curves 2 and 3, respectively). It is worth noting that the high intensity of the STE emission in the film is an indication of their sufficient structural perfection.

The luminescence spectra of CsI:Tl film and crystal with low (0.03%)  $\text{TI}^+$  content under excitation by SR in the range of interband transitions (13.75 eV) or in the range of A-absorption band of  $\text{TI}^+$  ions (4.5–4.28 eV) at 10 K (Figs. 3a and b, respectively) contain two emission bands peaked at

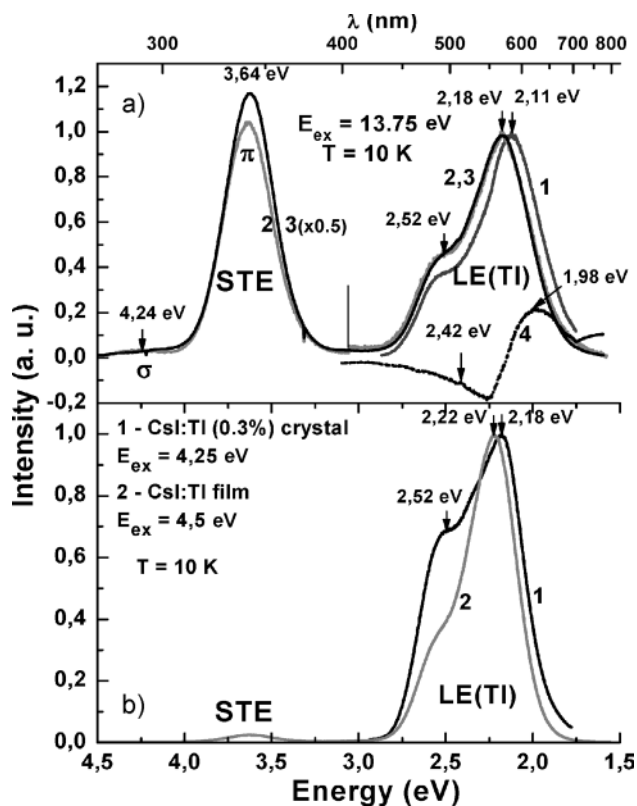


**Figure 3** Luminescence spectra of CsI:Tl film (3a, 2b) and CsI:Tl crystals (1a, 2a, 1b) with high (0.3%) (1a, 1b) and low (0.03%) (2a)  $\text{Ti}^+$  concentration under excitation by SR with an energy of 13.75 eV in the range of interband transitions (a) and 4.25 eV (1)/4.5 eV (2) in the A-absorption band (b) of  $\text{Ti}^+$  ions at 10 K. Curve 4a is the difference between the emission spectra 1a and 3a.

$E_{\text{max}} = 2.52$  and 2.22 eV, caused by  $\text{Ti}^+$  doping. This well-known luminescence of CsI:Tl compound is related to the radiative relaxation from the weak-off and strong-off configurations of localized excitons around  $\text{Ti}^+$  ions (LE(Tl) centers), respectively [16–19]. It is worth noting that the emission band related to the radiative intrinsic  $^3\text{P}_{1,0} \rightarrow ^1\text{S}_0$  transition of  $\text{Ti}^+$  ions is also present in the emission spectra of films and crystals in the 3.1–3.4 eV range, but the intensity of this emission at  $\text{Ti}^+$  concentration in the 0.03–0.3% range is so small that it can be seen only when using the logarithm scale.

The form of the luminescence spectra and position of the emission bands in CsI:Tl film are very close to those for CI:Tl crystal with low (0.03%) concentration of  $\text{Ti}^+$  ions (Fig. 3a, curves 3 and 2, respectively) which is evidence of the presence in these samples of the same set of emission centers created by the  $\text{Ti}^+$  ions. At the same time, the position (2.11 eV) of the strong-off emission band of LE(Tl) centers in CI:Tl crystal with high (0.3%) content of  $\text{Ti}^+$  ions under excitation at 13.75 eV at 10 K is markedly shifted to the long-wavelength range with respect to the position (2.18 eV) of the corresponding band in CI:Tl film and CI:Tl crystal with low (0.03%) concentration of  $\text{Ti}^+$  ions. Similar behavior takes place in the emission spectra of CI:Tl crystal and film

under excitation in the A-bands of  $\text{Ti}^+$  ions (Fig. 3b); specifically, we can observe the low-energy shift of the emission spectra of high-doped CI:Tl (0.3%) crystal (curve 1) with respect to low-doped film and crystal analogs (curve 2). This can be considered as an evidence of the existence of different types of the  $\text{Ti}^+$ -related centers in the high-doped CI:Tl (0.3%) crystal, which can additionally contribute to the luminescence in the visible range. Most probably, these centers are caused by formation of  $\text{Ti}^+$  dimer centers [19]. The formation of such centers is a typical phenomenon in doping of ionic crystals by mercury-like ions with electronic structure  $ns^2$ , which usually are characterized by very strong interaction with anions and cations of the host [19, 20].

The difference in the emission spectra of the high-doped CsI:Tl (0.3 at.%) crystal and the low-doped CsI:Tl film under high-energy excitation and excitation in the A-band of  $\text{Ti}^+$  ions are shown in Figs. 4b and a, respectively, by curves 3. The different concentration of the dimer centers in the crystals and films is reflected in the essential diversity of the shape of the corresponding differential emission spectra in Figs. 4b and a, curves 3. From these spectra, as well as from the differential spectrum 4 in Fig. 3a, we can estimate the position of the bands related to the  $\text{Ti}^+$  dimer centers in the high-doped CsI:Tl (0.3%) crystal. Namely, the positions of these bands can be estimated from the extremes of additional bands located around 2.38–2.41 and 1.98 eV in the difference spectra of the CsI:Tl (0.3%) crystal in comparison with same spectra for CsI:Tl film (Fig. 3a, curve 4 and Figs. 4b and a,

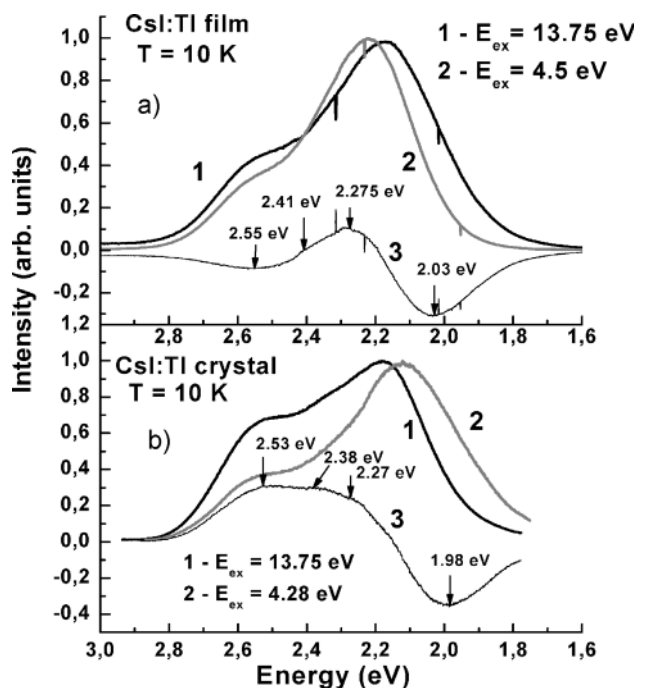


**Figure 4** Difference in the emission spectra under high-energy excitation at 13.75 eV (curves 1) and excitation at 4.3–4.5 eV in the A-band of  $\text{Ti}^+$  ions (curves 2) for CsI:Tl film (a) and crystal (b) at 10 K. Curves 3 present the difference in the emission spectra 1 and 2 in both fragments.

curves 3). Similarly to the 2.52 and 2.22 eV emission bands in Cl:Tl films and Cl:Tl crystal with low (0.03%) concentration of  $Tl^{+}$  ions, these emission bands in the high-doped Cl:Tl (0.3%) crystals can correspond to the weak-off and strong-off configuration of the excitons localized around the dimer  $Tl^{+}$  centers.

The excitation spectra of the STE and  $Tl^{+}$ -related luminescence in the visible range in Cl:Tl film and Cl:Tl (0.3%) crystal at 10 K are shown in Fig. 5. The structure of the  $\pi$ -component of the STE luminescence excitation spectra in the 5.5–7.0 eV and 7.5–8.5 eV ranges (Fig. 5c) represents, on the whole, the structure of the s- and d- states of I anions forming the bottom of the CsI conductive band [21]. The structure of the excitation spectra of the weak-off luminescence of LE(Tl) centers in the CsI:Tl film and crystal in the 4.2–5.5 eV range is completely similar and contains the set of strongly overlapped A (doublet), B (doublet) and C (triplet) bands that can correspond to the intrinsic  $^1S_0 \rightarrow ^3P_1, ^3P_2, ^1P_1$  radiative transition of  $Tl^{+}$  ions with electronic structure  $ns^2$ . The positions of all the mentioned bands in CsI:Tl film are summarized in Table 2.

The structure of the excitation spectra of the strong-off luminescence in CsI:Tl film and crystal at 10 K (Fig. 5b, curves 1 and 2, respectively) is not identical and is significantly changed with respect to the excitation spectra of the weak-off emission (Fig. 5a). Specifically, the finely

**Table 2** Position of bands in the excitation spectra of different  $Tl^{+}$  centers in CsI:Tl films.

type of band (eV)	A <sub>1</sub>	A <sub>2</sub>	B <sub>1</sub>	B <sub>2</sub>	C <sub>1</sub>	C <sub>2</sub>	C <sub>3</sub>
strong-off LE(Tl)	4.27	4.5	4.64	4.8	5.02	5.20	5.38
weak-off LE(Tl)	4.26	4.47	4.66	4.8	4.97	5.15	5.38

structured bands, corresponding to the respective radiation transitions between the  $^1S_0$  ground state and excited  $^3P_1, ^3P_2$ , and  $^1P_1$  levels of  $Tl^{+}$  ions are overlapped with the strong wide bands in the 3.9–4.65 and 4.65–5.5 eV ranges. Most probably, these bands correspond to the charge-transfer transitions (CTT) [22] between the states of  $I^{-}$  anions, forming the top of the CsI:Tl valence band, and  $Tl^{+}$  ions as well as  $Tl^{+}$  ions and the bottom of conduction band. The intensity of these bands increases with the rise of  $Tl^{+}$  concentration and their position shifted to the low-energy range. Specifically, the intensity of CTT bands is larger in CsBr:Tl (0.3%) crystal and position of their low-energy edge (4.09 eV) is significantly shifted in the low-energy range with respect to the corresponding value 4.27 eV in CsI:Tl film. Most probably, such a shift of the excitation spectra of the visible emission in the high-doped CsI:Tl crystal is caused by overlapping the excitation spectra of the strong-off luminescence of excitons localized around  $Tl^{+}$  single and dimer centers.

Thus, based on the comparative analysis of the emission spectra of CsI:Tl films and crystals with different  $Tl^{+}$  content we have concluded that the dominant mechanism of excitation of the strong-off LE(Tl) luminescence is the CTT between  $I^{-}$  anions and the excited states of  $Tl^{+}$  single and dimer centers.

The decay kinetics of the weak-off and strong-off luminescence of LE(Tl) centers under high-energy excitation above bandgap of the CsI host is presented in Fig. 6a. All decay curves show the two-component structure of the luminescence [6–9] with the decay times of fast components in the 2.4–3.3 ns range and slow components in the tens of  $\mu s$  ranges, corresponding to the radiative transition from the singlet and triplet excited states of LE(Tl) centers [16–19]. However, due to the high repetition frequency of SR pulse and narrow observation time gate (200 ns) the decay times of the longer components of  $Tl^{+}$  emission cannot be determined by the setup used. At the same time, from the respective approximation of the decay curves in Fig. 6, we can see that the decay kinetics of the main slow component of the weak-off luminescence of LE(Tl) centers (Fig. 6, curves 1 and 2) is faster than that of the main component of the strong-off luminescence (Fig. 6, curves 3 and 4), which indicates their different origin of the corresponding radiative transitions [16–19].

From Fig. 6 is also seen that the CsI:Tl film under excitation in the range of the interband transitions have somewhat faster decay kinetics of the weak-off luminescence of LE(Tl) centers (curve 2) in comparison with the high-doped CsI:Tl (0.3%) crystal (curve 1). However, due to

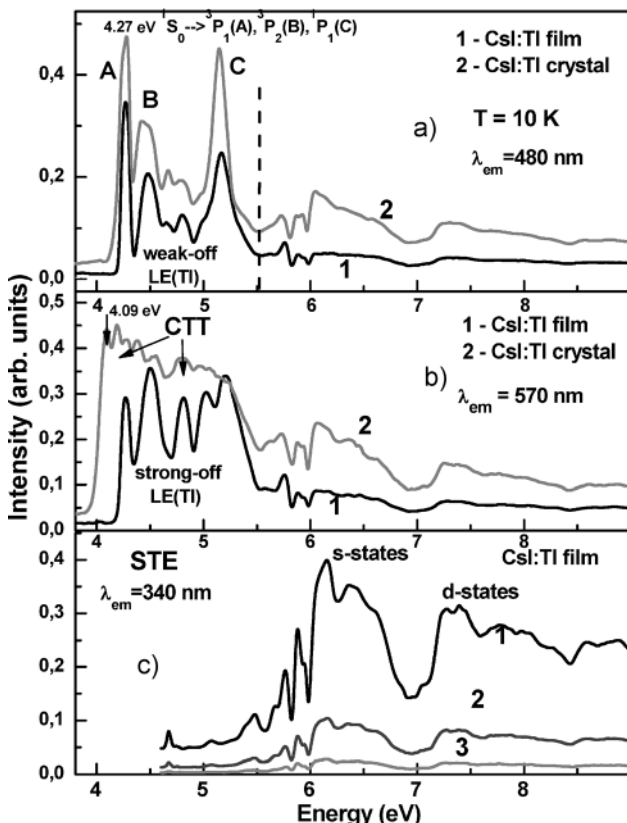


**Figure 5** Excitation spectra LE(Tl) luminescence (a, b) in the bands peaked at 2.52 (a) and 2.18 eV (b) in CsI:Tl film (1) and CsI:Tl (0.3%) crystal (2) at 10 K. c) STE spectra presenting the states of I ions.

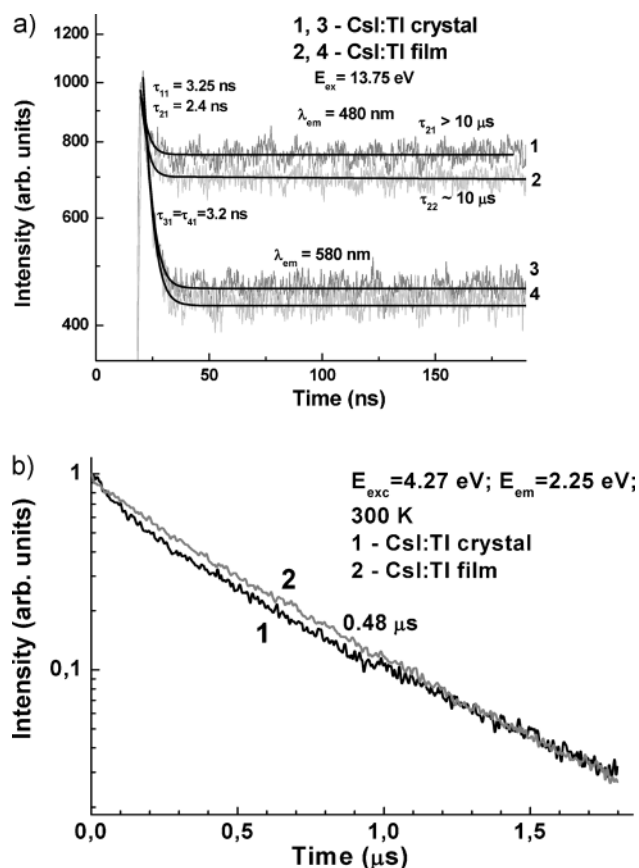


**Figure 6** (a) Decay kinetics of LE(Tl) centers luminescence of CsI:Tl crystals (1, 3) and films (2, 4) at 10 K under excitation by SR with an energy of 13.75 eV in the range of interband transitions. Two-component exponential fits of decay curves are given by solid lines. (b) Decay kinetics of luminescence of CsI:Tl crystals (1) and films (2) at 300 K under excitation in A-band of  $\text{TI}^+$  ions at 4.27 eV and registration of luminescence at 2.25 eV.

the narrow observation time gate (200 ns) we can only correctly estimate the fast (in the tens ns range) components of LE(Tl) emission in these samples, while the longer components (calculated decay time above 10  $\mu\text{s}$ ) can not be well evaluated. Therefore, we also measured the decay kinetics of the weak-off luminescence of LE(Tl) centers at 2.25 eV in CsI:Tl (0.3%) crystal and films under excitation at 4.27 eV in the A-band band of  $\text{TI}^+$  ions (Fig. 6b). As can be seen from Fig. 6, curve 1 the decay kinetics of the LE(Tl) center luminescence in CsI:Tl film is close to a single-exponential decay with a decay time of 0.48  $\mu\text{s}$ . As opposed to the film, the decay kinetics of the LE(Tl) luminescence in the CsI:Tl (0.3%) crystal is nonexponential and visibly slower than that in the film. Most probably, the differences in the decay kinetics of the weak-off luminescence of LE(Tl) centers in CsI:Tl film and crystal are caused by the different concentrations of the  $\text{TI}^+$  single and dimer centers because the relative concentration of these centers and the total content of  $\text{TI}^+$  ions are peculiar to crystallization of these phosphors by the LPE and Stockbarger–Bridgman methods.

**4 Conclusions** CsI:Tl films have been crystallized by the LPE method from the CsI:Tl (0.3 mol.%) crystalline salt onto substrates from undoped CsI crystals. We have found that the segregation coefficient of  $\text{TI}^+$  ions at SCF crystallization (0.008–0.12) is lower by about one order of magnitude than the corresponding value of 0.75 for CsI:Tl (0.03–0.3 mol.%) crystals grown from melt by the Stockbarger–Bridgman method.

The LY of the luminescence of the CsI:Tl (0.3%) films grown by LPE amounts to  $\sim 75$ –82% of that for CsI:Tl (0.3%) crystal under excitation by  $\alpha$  particles of  $\text{Pu}^{239}$  (5.15 MeV) sources. At the same time, the energy resolution (FWHM, %) of these films (19.1–22.3%) is lower than that for CsI:Tl (0.3%) crystals (6.5%) due to somewhat lower structural homogeneity of the films.

The luminescent properties of the CsI:Tl films are compared with the corresponding properties of CsI:Tl (0.3 and 0.03%) crystals grown from the melt under excitation by SR with an energy of 3.7–9 eV. The luminescence of the CsI:Tl (0.03%) crystal and CsI:Tl film in the visible spectral range in the bands peaked at  $E_{\text{max}} = 2.52$  and 2.22 eV is related to the radiative relaxation from the weak-off and strong-off configurations of excitons localized around  $\text{TI}^+$  ions (LE(Tl) centers), respectively. We have shown that in the high-doped CsI:Tl (0.3%) crystal formation of the  $\text{TI}^+$  dimer centers can take place. Namely, the additional visible emission bands peaked approximately at 2.42 and 1.98 eV can be related to the weak-off and strong-off configuration of excitons localized around the  $\text{TI}^+$  dimer centers.

We have found that the dominant mechanism of excitation of the strong-off luminescence of the LE(Tl) centers is the charge transfer transition between the  $\Gamma$  anion and the  $\text{TI}^+$  ions as well as the  $\text{TI}^+$  ions and the bottom of conduction band in both single and dimer centers.

CsI:Tl films have somewhat faster kinetics of the luminescence decay under excitation in the range of interband transitions in comparison with the bulk crystal analogs, prepared from the same salt, due to differences in the concentration of the  $\text{TI}^+$  single and dimer centers that are peculiar to crystallization of these phosphors by the LPE and Bridgman methods.

**Acknowledgements** The authors express their gratitude to Dr. W. Drube and Dr. A. Kotlov for their assistance in carrying out the experiments in HASYLAB at DESY. The work was fulfilled in the framework of HASYLAB II-20090087 research projects and Ministry of Education and Science of Ukraine project SL-28 F.

## References

- [1] T. Martin and A. Koch, *J. Synchr. Rad.* **13**, 180 (2006).
- [2] M. Globus and B. Grinyov, *Non-organic Scintillators. New and Traditional Materials* (Akta, Kharkiv, 2000).
- [3] A. Ananenko, A. Fedorov, P. Mateychenko, V. Tarasov, and Yu. Vidaj, *Appl. Surf. Sci.* **236**, 186 (2004).
- [4] A. Fedorov, A. Lebedinsky, and O. Zelenskaya, *Nucl. Instrum. Methods Phys. Res. A.* **564**, 328 (2006).
- [5] V. V. Nagarkar, V. Gaysinskiy, I. Shestakova, and S. Taylor, *IEEE Nucl. Sci. Symp. Conf. Rec.* **5**, 3334 (2004).

- [6] V. V. Nagarkar, V. Gaysinskiy, E. E. Ovechkina, S. C. Thacker, S. R. Miller, C. Brecher, and A. Lempicki, *IEEE Nucl. Sci. Symp. Conf. Rec.* **6**, 3567 (2006).
- [7] V. V. Nagarkar, V. Gaysinskiy, E. E. Ovechkina, S. C. Thacker, S. R. Miller, C. Brecher, and A. Lempicki, *IEEE Trans. Nucl. Sci.* **54**, 1378 (2007).
- [8] Bo Kyung Cha, Jeong-Hyun Shin, Jun Hyung Bae, Chae-hun Lee, Sungho Chang, Hyun Ki Kim, Chan Kyu Kim, and Gyuseong Cho, *Nucl. Instrum. Methods Phys. Res. A* **604**, 224 (2009).
- [9] Yu. Zorenko, V. Gorbenko, I. Konstankevich, A. Voloshinovskii, G. Stryganyuk, V. Mikhailin, V. Kolobanov, and D. Spassky, *J. Lumin.* **114**, 85 (2005).
- [10] Yu. Zorenko, I. Konstankevych, V. Gorbenko, and T. Zorenko, *Mol. Phys. Rep.* **36**, 127 (2002).
- [11] Yu. V. Zorenko, R. M. Turchak, T. I. Voznyak, and A. P. Luchechko, *J. Appl. Spectrosc.* **73**, 211 (2006).
- [12] M. Globus, B. Grinyov, M. Ratner, V. Tarasov, V. Lyubinskiy, Y. Vydai, A. Ananenko, Y. Zorenko, V. Gorbenko, and I. Konstankevych, *IEEE Trans. Nucl. Sci.* **51**, 1297 (2004).
- [13] M. Kh. Ashurov, Yu. K. Voronko, V. V. Osiko, and A. A. Sobol, *Phys. Status Solidi A* **42**, 101 (1977).
- [14] M. M. Kuklja, *J. Phys.: Condens. Matter* **12**, 2953 (2000).
- [15] <http://abulafia.mt.ic.ac.uk/shannon/radius.php>
- [16] V. Nagirnyi, S. Zazubovich, V. Zelepin, M. Nikl, and G. P. Pazzi, *Chem. Phys. Lett.* **227**, 533 (1994).
- [17] V. Nagirnyi, A. Stolovich, S. Zazubovich, V. Zelepin, E. Mihokova, M. Nikl, G. P. Pazzi, and L. Salvini, *J. Phys.: Condens. Matter* **7**, 3637 (1995).
- [18] V. Babin, K. Kalder, A. Krasnikov, and S. Zazubovich, *J. Lumin.* **96**, 75 (2002).
- [19] G. P. Pazzi, M. Nikl, M. Bacci, E. Mihokova, J. Hlinka, P. Fabeni, and L. Salvini, *J. Lumin.* **60/61**, 527 (1994).
- [20] V. Babin, V. Bichevin, V. Gorbenko, A. Makhov, E. Mihokova, M. Nikl, A. Vedda, S. Zazubovich, and Yu. Zorenko, *Phys. Status Solidi B* **246**, 1318 (2009).
- [21] Ch. B. Lushchik and A. Lushchik, *Decay of Electronic Excitation with Defect Formation in Solids* (Nauka, Moscow, 1989).
- [22] P. Dorenbos, *J. Phys.: Condens. Matter* **15**, 8417 (2003).